NASA Technical Memorandum 103674

Effect of Hydrogen on the Strength and Microstructure of Selected Ceramics

Thomas P. Herbell, Andrew J. Eckel,
and David R. Hull
National Aeronautics and Space Administration
Lewis Research Center
Cleveland, Ohio

and

Ajay K. Misra
Sverdrup Technology, Inc.
Lewis Research Center Group
Brook Park, Ohio

Prepared for the
Fall Meeting of the Metallurgical Society
Detroit, Michigan, October 7–11, 1990

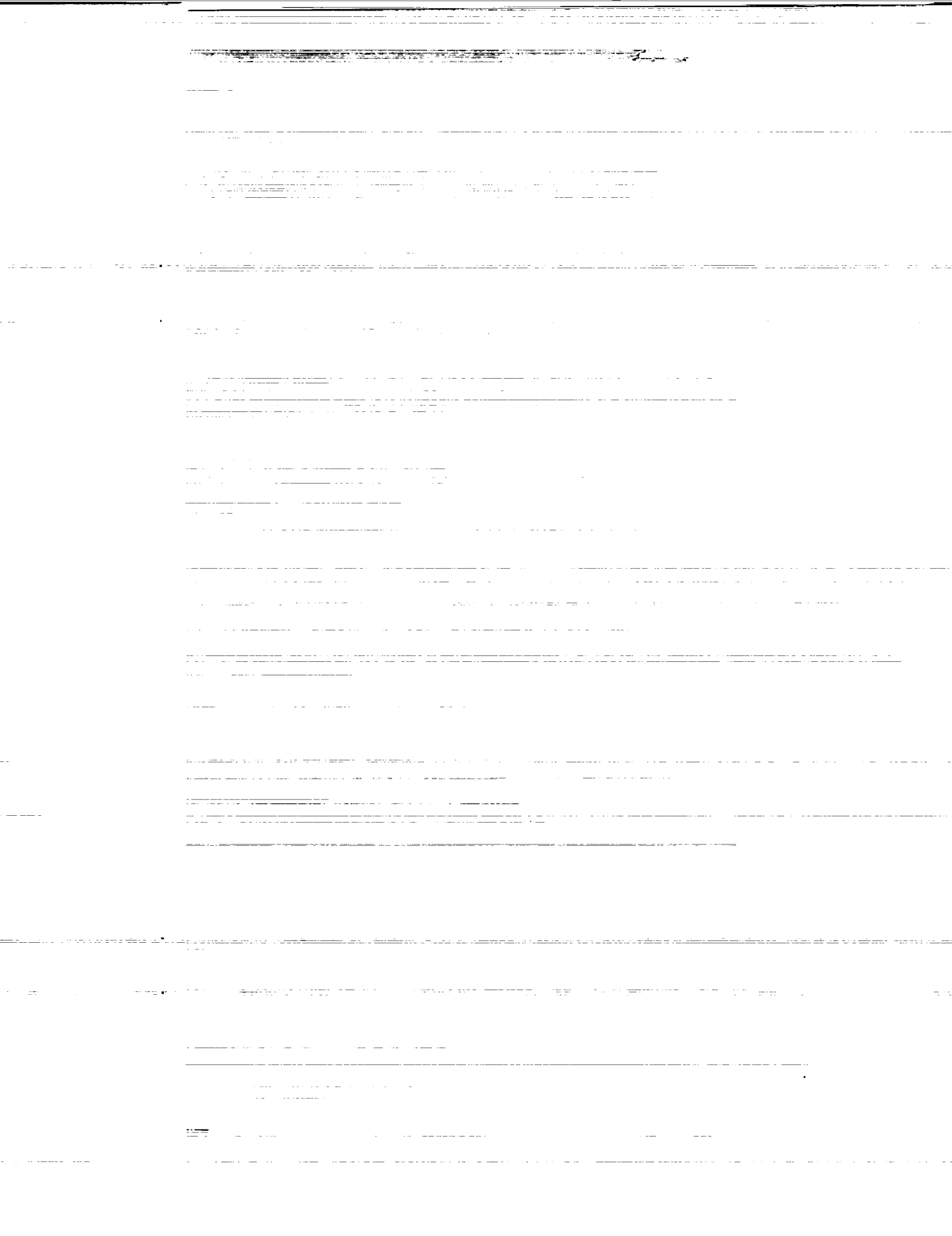

EFFECT OF HYDROGEN ON THE STRENGTH AND MICROSTRUCTURE OF SELECTED CERAMICS

Thomas P. Herbell, Andrew J. Eckel, and David R. Hull

NASA Lewis Research Center
Cleveland, Ohio 44135

and

Ajay K. Misra

Sverdrup Technology Inc.
Lewis Research Center Group
Brook Park, Ohio 44142

Abstract

Ceramics in monolithic form and as composite constituents in the form of fibers, matrices, and coatings are currently being considered for a variety of high-temperature applications in aeronautics and space. Many of these applications involve exposure to a hydrogen-containing environment. This study assesses the compatibility of selected ceramics in gaseous high-temperature hydrogen. Environmental stability regimes for the long term use of ceramic materials are defined by the parameters of temperature, pressure, and moisture content. Thermodynamically predicted reactions between hydrogen and several monolithic ceramics are compared with actual performance in a controlled environment. Morphology of hydrogen attack and the corresponding strength degradation is reported for silicon carbide, silicon nitride, alumina, magnesia, and mullite.

Introduction

Elevated temperature compatibility and hydrogen permeability of ceramics will be critical factors for their use in monolithic form and as composite constituents in metal matrix composites (MMC), carbon/carbon (C/C), and ceramic matrix composites (CMC). As an example, aluminide matrix composites will form alumina (Al_2O_3) scales in oxygen, and alumina is a promising fiber candidate for these composites. Silicon carbide (SiC) and silicon nitride (Si_3N_4) have been considered as protective coatings for C/C, for reinforcing fibers in MMC and CMC, and for matrices in CMC. Magnesium oxide (MgO) and mullite ($3Al_2O_3 \cdot 2SiO_2$) are being considered as fibers and as matrices for oxide composites. These materials - SiC, Si_3N_4, Al_2O_3, MgO, and mullite - and/or the scales that form on them, must be stable in their proposed hydrogen use environments.

The objectives of this study are to report the thermodynamics of hydrogen (H_2) attack on the selected pure ceramics (SiC, Si_3N_4, Al_2O_3, MgO, and mullite), to compare thermodynamic predictions with actual performance of commercial polycrystalline ceramics, to determine the morphology of attack (if any), and to measure room temperature strength degradation of exposed samples.

Experimental Procedure

Thermodynamic Analysis

The chemical stability of a large number of ceramic materials in H_2-containing environments has been analyzed from thermodynamic considerations by Misra (1). Equilibrium calculations were made as a function of temperature (900 to 1400°C), total system pressure (1 to 30 atm), and moisture content (0 to 50 vol.%).

All of the equilibrium calculations were performed with the computer program SOLGASMIX-PV originally developed by Eriksson (2) and later modified by Besman (3). The program is based on the minimization of the Gibbs free energy of the system. For the calculations involving moisture, vapor pressures of the various species were calculated as a function of the ratio P_{H_2}/P_{H_2O}. An estimation of the upper use temperature of various ceramic materials is based on the arbitrary vapor pressure level of 10^{-6} atm of reaction product. In some applications, however, higher or lower levels of reaction product may be acceptable.

Hydrogen Effects Measurements

Ceramic test bars 6 by 3 by 25 mm were prepared by diamond grinding. The surface finish was less than or equal to 8 micro-inch rms. Before each H_2 exposure, the bars were ultrasonically cleaned in neat ethanol and were dried, measured, and weighed. Approximately 20 test bars were used in each H_2 test except for the mullite exposures which were limited to four bars for each test condition.

The H_2 gas was purified to an oxygen level of 2 ppm, and the purified gas was passed through a water bubbler, which essentially saturated the gas with water vapor at room temperature (2.9 volume percent H_2O). The flow rate was regulated at room temperature and held constant at 475 cm^3/min. Specimens were exposed to H_2 in a resistance-heated, horizontal tube furnace equipped with a 99.8 percent pure Al_2O_3 tube. The specimens were placed on high-purity Al_2O_3 setters in a high purity Al_2O_3 boat located in the central hot zone of the furnace. The temperature variation within the furnace hot zone was about ±10 °C.

The specimens were heated to the exposure temperature in high-purity helium. Once the desired temperature was achieved, the atmosphere was switched to wet H_2 by direrting the gas through a bubbler. The samples were exposed to the wet H_2 for 100 h at temperatures up to 1400°C. At the completion of the exposure cycle, the gas was again switched to helium for the cool-down cycle.

After the H_2 exposure, the samples were removed from the furnace, weighed, and measured. The exposed specimens were subsequently stressed to fracture in a four-point bend fixture. The loading rate was 0.05 cm/min with an outer span of 1.90 cm and an inner span of 0.95 cm. The following equation was used to calculate fracture strength (MOR):

$$\text{MOR strength} = 3P(L - a)/2bd^2 \quad (1)$$

where P is the load at failure, L is the outer span, a is the inner span, b is the specimen width, and d is the specimen thickness. The post-exposure dimensions were used to calculate the fracture stresses.

Surface of exposed samples were examined by scanning electron microscopy (SEM), x-ray energy dispersive spectroscopy (XEDS), and optical microscopy. Fractography of broken bars is currently under way and is not included in this paper.

Results and Discussion

Silicon Carbide

Thermodynamic Stability of Silicon Carbide in Hydrogen. Thermodynamic calculations show that SiC will decompose in pure H_2. This is consistent with results reported in the literature (4-6). Figure 1 shows the equilibrium partial pressure of reaction product gases for reaction of SiC with pure H_2 at 1-atm pressure. Although there are other possible gaseous species, calculations show that CH_4, SiH, and SiH_4 are predominant. The only stable solid phase is silicon (Si).

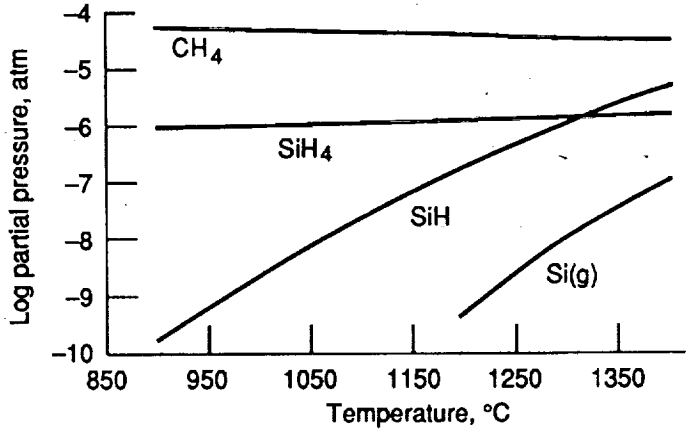

Figure 1-Equilibrium partial pressures of reaction product gases for reaction of SiC with pure H_2 at 1 atm.

Since the partial pressures of the Si-H species are at least an order of magnitude less than that of CH_4 for these conditions, the primary reaction is the decomposition of SiC:

$$SiC + 2H_2 = Si + CH_4 \quad (2)$$

The partial pressure of all three gaseous species -- CH_4, SiH, and SiH_4 -- increases with increasing system pressure. Thus, SiC would be expected to decompose at an increasing rate with increasing total system pressure in an environment of pure H_2.

The stability of SiC in the presence of moisture is characterized by distinct regions of attack. Each region is defined by the thermodynamically stable solid phases. The calculated partial pressures of the major gaseous species and the stable condensed phases at 1400°C are shown in Figure 2.

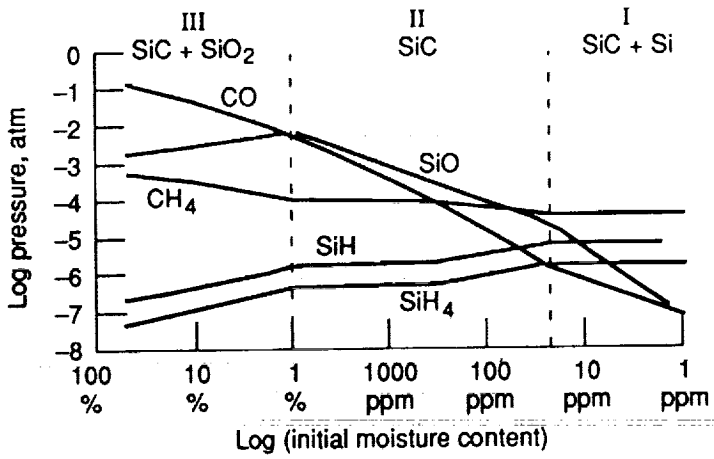

Figure 2-Stability of SiC in $H_2 + H_2O$ at 1 atm and 1400°C.

In Region I, the stable solids are Si and SiC. This region is similar to that previously discussed for SiC in pure H_2 in that the predominant vapor species is CH_4, which forms as a result of the decomposition of SiC. This is the same as that described by Equation (2).

Region II is identified by the single, stable, solid phase of SiC. This is the region of active attack of the SiC where the volatile suboxide SiO rather than the solid, protective SiO_2 is formed. Region III is the region of passive oxidation: the stable solid species being SiC and SiO_2. Formation of SiO_2 is likely to provide protection against further oxidation. The effectiveness of the SiO_2 scale in inhibiting further oxidation would depend on the morphology and stability of the scale formed.

Morphology of Hydrogen Attack on Silicon Carbide. To predict a material's performance in a particular environment one must understand both the thermodynamics and kinetics of reactions that may occur, as well as the morphology that results from such reactions. [(Kinetic information for SiC-H_2 reactions is reported elsewhere (7)]. Scanning electron microscopy was used to analyze the surface morphological characteristics of samples in the as-received condition and after exposure to two levels of wet H_2 at 1300°C. The moisture levels were selected to be from thermodynamically predicted Regions II and III of Figure 2, since these are the regions of practical interest. The microstructures are shown in Figure 3. Figure 3a shows the surface of the as-received sintered α-SiC, revealing grinding marks and surface damage. After exposure at an intermediate moisture level (Region II), active attack of the SiC grains is observed (Figure 3b). At high moisture levels (Region III), a protective SiO_2 scale forms on the surface of the SiC (Figure 3c). This protective SiO_2 scale has previously been observed by other researchers for SiC in other oxidizing environments (8, 9).

Post-Exposure Strength of Silicon Carbide. Test bars of sintered α-SiC exposed to wet H_2 (saturated with moisture at room temperature) for 100 h at temperatures to 1400°C were tested at room temperature to evaluate the effect of high-temperature exposure on residual room temperature strength. This moisture level falls within the previously described Region III where passive oxidation to form SiO_2 on the surface would be expected. As can be seen in Figure 4, essentially no degradation of room temperature flexural strength was observed. Longer exposure times in dry H_2 have, however, been observed to degrade the strength of this material (5).

Silicon Nitride

Thermodynamic Stability of Silicon Nitride in Hydrogen. Thermodynamic calculations show that the reaction of Si_3N_4 with pure H_2 will lead to the formation of pure Si along with the generation of N_2, NH_3, SiH, and SiH_4 as the major gaseous products. The partial pressures of these species as a function of temperature are shown in Figure 5. At temperatures above about 1200°C, the partial pressure of N_2 is an order of magnitude greater than those of SiH_4 and SiH. Therefore at these temperatures the predominant product species would be N_2. This suggests that at high temperatures Si_3N_4 decomposes to Si and N_2 according to the reaction

$$Si_3N_4 = 3Si + 2N_2 \quad (3)$$

Thus pure H_2 would not be expected to play a major chemical role in the degradation of Si_3N_4 at high temperatures.

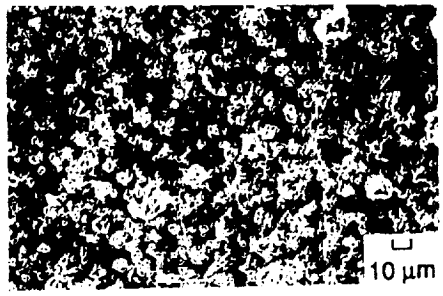

(a) As received.

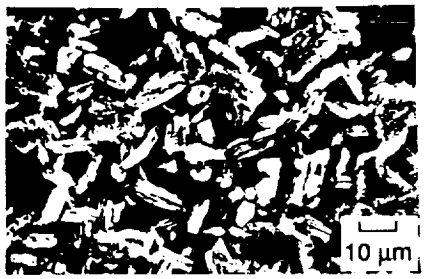

(b) Region II, active attack.

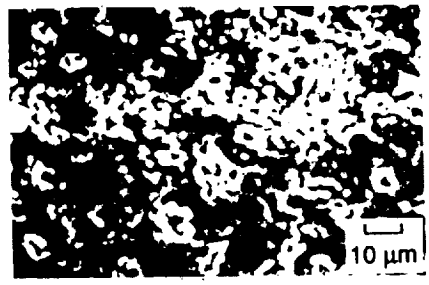

(c) Region III, protective SiO_2 formation.

Figure 3-Surface morphology of α-SiC exposed to hydrogen at 1300°C.

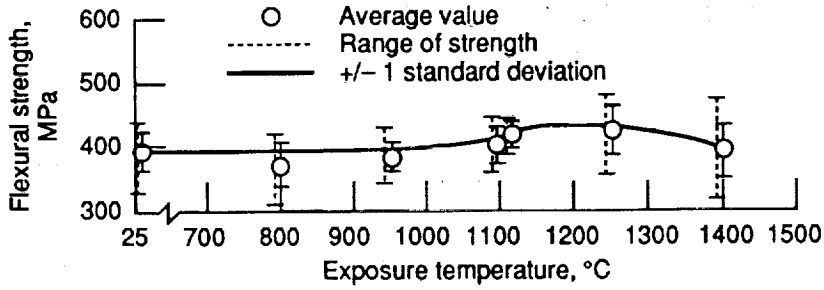

Figure 4-Effect of elevated temperature H_2 exposure (100 h in Region III) on room temperature strength of sintered α-SiC.

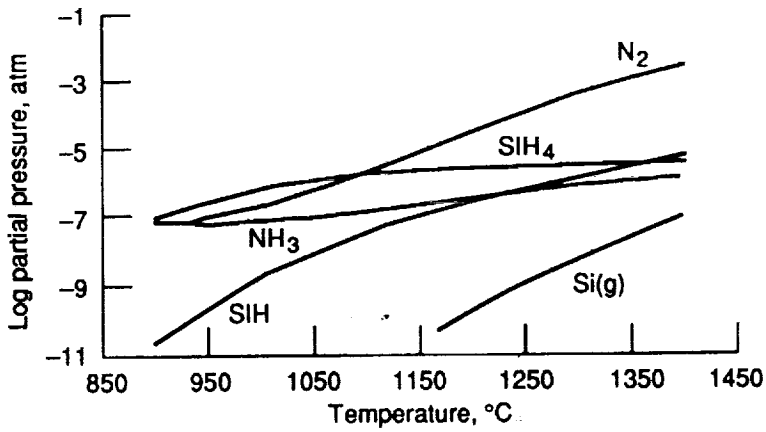

Figure 5-Equilibrium partial pressures of reaction product gases for reaction of Si_3N_4 with pure H_2 at 1 atm.

At lower temperatures (<1100°C), degradation of Si_3N_4 is probably due to the reaction with H_2 resulting in the formation of SiH_4 and the release of N_2:

$$Si_3N_4 + 6H_2 = 3SiH_4 + 2N_2 \quad (4)$$

As was the case for SiC at 1400°C, the stability of Si_3N_4 in the presence of moisture is characterized by three distinct stability regimes. Once again each region is defined by the thermodynamically stable solid phases. The calculated partial pressures of the major gaseous species and the stable condensed phases present at 1400°C are seen in Figure 6.

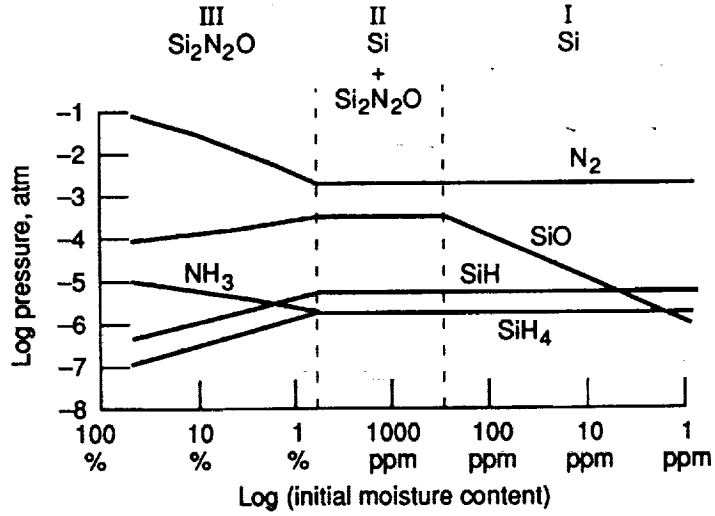

Figure 6-Stability of Si_3N_4 in $H_2 + H_2O$ at 1 atm and 1400°C.

In Region I, the stable solids are Si and Si_3N_4, with N_2 being the predominant gas. The primary mode of reaction in Region I is the decomposition of Si_3N_4 into Si and N_2, which is the same as for reaction with pure H_2. Hydrogen and moisture have little effect on the decomposition in this region. At intermediate moisture levels, Region II, the stable solid phases are Si, Si_3N_4, and Si_2N_2O. The decomposition of Si_3N_4 is probably similar to that in Region I.

At higher moisture contents, Region III, the equilibrium solid phases are Si_3N_4 and Si_2N_2O. On the basis of the stability of Si_2N_2O in H_2-H_2O atmospheres, the Si_2N_2O would be expected to convert to SiO_2. Therefore, the predicted oxide scale on Si_3N_4 in Region III would consist of an outer layer of SiO_2 and an inner layer of Si_2N_2O next to the Si_3N_4 surface. The integrity of the SiO_2 scale would control the rate of reaction in this region.

Morphology of Hydrogen Attack on Silicon Nitride. Verification of thermodynamics for Si_3N_4 in Region III has been provided by many researchers. This is the region of passive oxidation where a protective surface oxide layer forms. Similar to Figure 3a, the as-received Si_3N_4 also shows grinding marks and some surface damage (Figure 7a). An example of a complex silica-based protective oxide layer that forms on a commercial sintered Si_3N_4 at high temperatures in an oxidizing environment is shown in Figure 7b. This complex structure results from the addition of sintering aids used in the fabrication of this material, including 10 percent yttria (Y_2O_3) and 2 percent strontia (SrO).

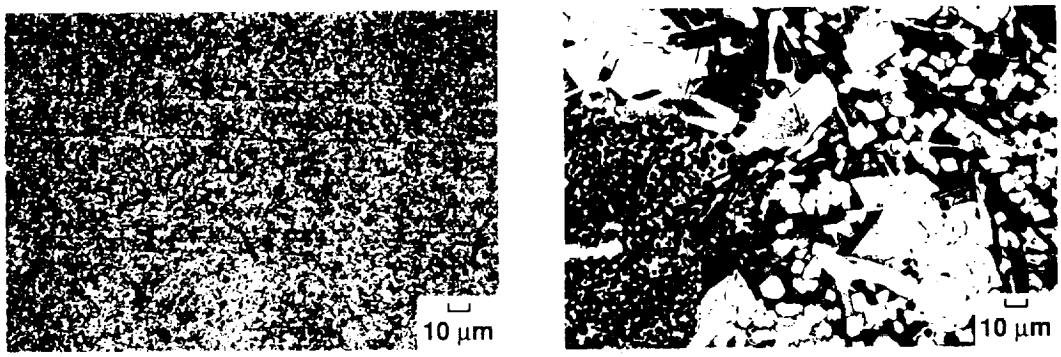

(a) As received.

(b) Exposed 100 h in hydrogen at 1300°C (Region III).

Figure 7-Surface morphology of Si_3N_4.

Post-Exposure Strength of Silicon Nitride. Test bars of the sintered Si_3N_4 were exposed to wet H_2 for 100 h at temperatures to 1400°C. As with SiC, the moisture level used falls within Region III where passive oxidation of the Si_3N_4 is expected. Figure 8 shows that strength drops off after exposure to temperatures greater than 1200°C. Similar behavior has been noted for Si_3N_4 exposed to non-H_2-containing atmospheres. This strength loss is presumably due to degradation of the protective SiO_2-based scale on the surface of the Si_3N_4.

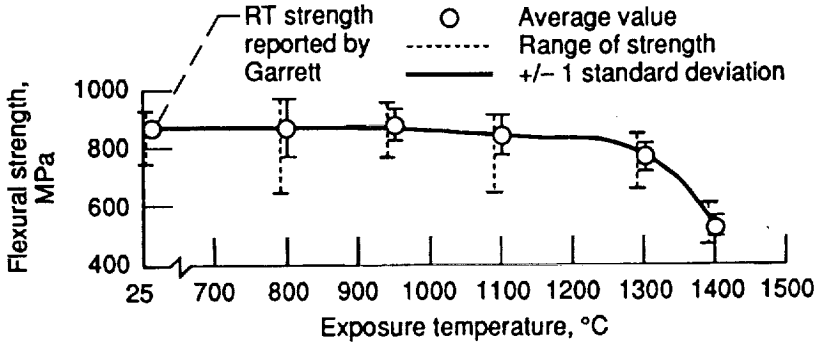

Figure 8-Effect of elevated temperature H_2 exposure (100 h) on room temperature strength of sintered Si_3N_4.

Aluminum Oxide

Thermodynamic Stability of Aluminum Oxide in Hydrogen. Equilibrium calculations show that Al_2O_3 is the only condensed phase in equilibrium with H_2. The predominant gaseous species are Al(g) and Al_2O(g). Al(g) is expected to predominate because its partial pressure is an order of magnitude greater than that of Al_2O. The equilibrium partial pressure of Al(g) as a function of total system pressure for Al_2O_3-H_2 equilibria is shown in Figure 9. This figure indicates that at 1 atm pressure Al_2O_3 is quite stable in pure H_2. Although the stability decreases with increased pressure at all temperatures, system pressure has essentially a negligible effect on the stability of Al_2O_3 in H_2.

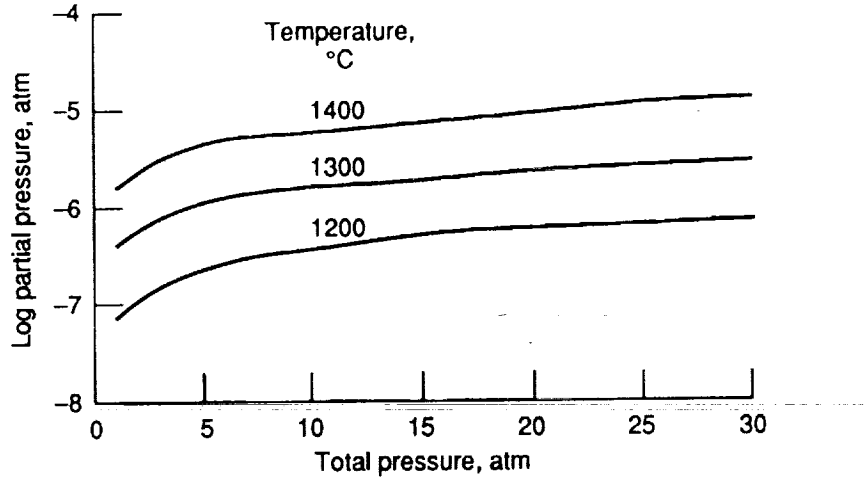

Figure 9-Equilibrium partial pressure of Al(g) as a function of total pressure for Al_2O_3-H_2 system.

Figure 10 shows the equilibrium partial pressures of various product gases for the reaction of Al_2O_3 in H_2+H_2O at 1400°C and 1 atm. Al_2O_3 is the only stable condensed species and Al(g) is the predominant gaseous reaction product. Even at very low moisture levels, the partial pressure of Al(g) is low. And for moisture contents greater than 10 ppm, the equilibrium partial pressure of Al(g) decreases with increasing moisture content. These calculations indicate that Al_2O_3 is expected to be very stable in H_2 and H_2+H_2O environments at high temperatures.

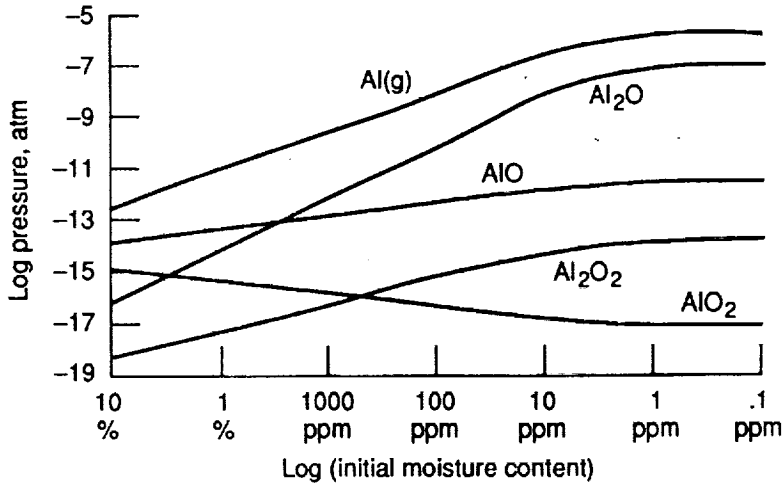

Figure 10-Equilibrium partial pressures of reaction product gases as a function of H_2O for Al_2O_3 + H_2 at 1 atm and 1400°C.

Morphology of Hydrogen Attack on Aluminum Oxide. The effects of high-temperature wet H_2 on the surface morphology of Al_2O_3 are seen in Figure 11. Figure 11a shows the typical grain size and structure of commercial sintered Al_2O_3. After exposure for 100 h at 1400°C, rosettes are seen to form on the surface (Figure 11b). Similar surface structure is seen on nickel aluminides exposed to oxidizing environments (10) and may be related to phase transitions in the Al_2O_3 surface.

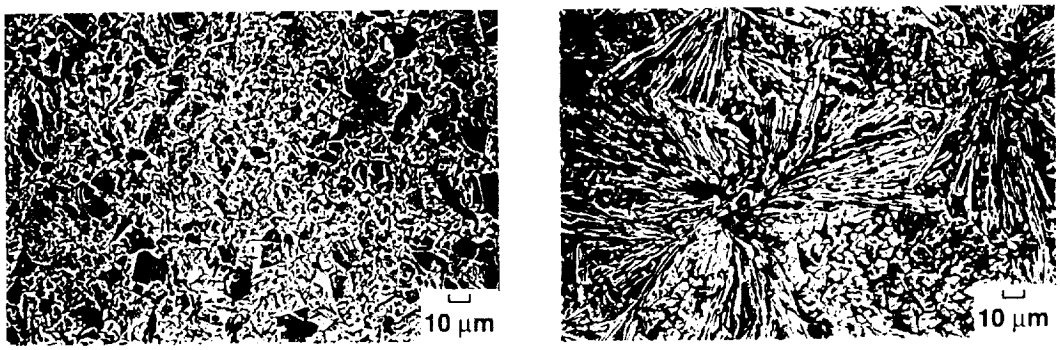

(a) As received.

(b) Exposed 100 h in wet hydrogen at 1400°C.

Figure 11-Surface morphology of Al_2O_3.

Post-Exposure Strength of Aluminum Oxide. Thermodynamically, Al_2O_3 is expected to be stable in the wet H_2 environment evaluated in this study. However, the post-exposure, room temperature flexural strength decreased approximately 20 percent (341 to 278 MPa) following a 100 h exposure to wet H_2 at 1400°C. This decrease may be related to the changes in flaw morphology as discussed above. These microstructural changes are being further investigated because they may significantly influence the upper use temperature for alumina as a structural material.

Magnesium Oxide

Thermodynamic Stability of Magnesium Oxide in Hydrogen. Thermodynamic calculations show that Mg(g) is the predominant reaction product for MgO in H_2 + H_2O environments. The relevant reaction is

$$MgO + H_2 = Mg(g) + H_2O \quad (5)$$

and equilibrium partial pressure of Mg(g) can be calculated from the expression

$$\log(P_{Mg}) = \log(K_5) + \log (P_{H_2}/P_{H_2O}) \quad (6)$$

The equilibrium partial pressures of Mg(g) as a function of moisture content are shown in Figure 12 for a total pressure of 1 atm. The partial pressure of Mg increases with increasing temperature and decreases with increasing moisture content. The total system pressure has no significant effect on the stability of MgO in H_2 + H_2O environments.

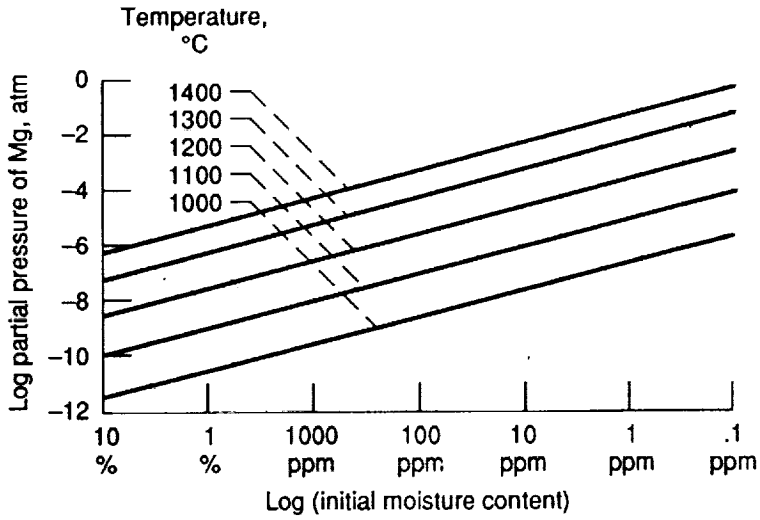

Figure 12-Partial pressure of Mg(g) as a function of moisture content and temperature for reaction of MgO with $H_2 + H_2O$ for a total pressure of 1 atm.

Morphology of Hydrogen Attack on Magnesium Oxide. The surface of as-received commercial MgO is shown in Figure 13a. The surface remained essentially unchanged (except for a coarsening of the grain structure) up to 1200°C. At 1400°C (Figure 13b), H_2 attack of the MgO grains is evident and large SiO_2-rich regions (marked "A") are seen. Energy dispersive x-ray analysis indicated these may be $MgO\text{-}SiO_2\text{-}CaO$ ternary silicates. SiO_2 and CaO ares present in the starting MgO, probably as a sintering aids.

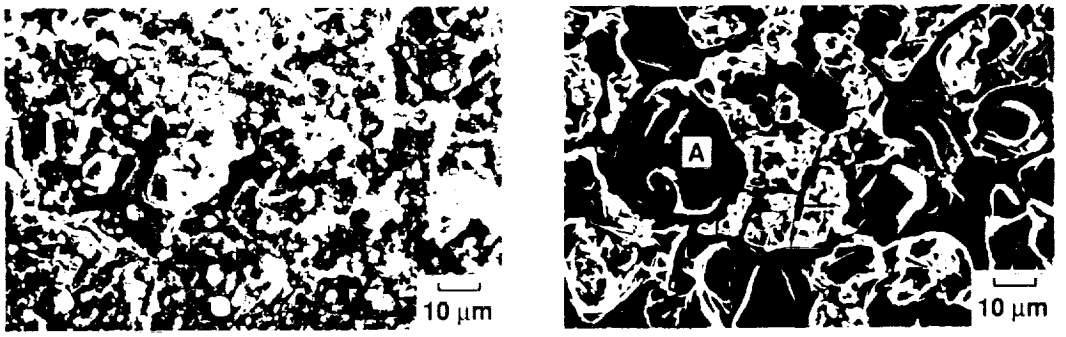

(a) As received.

(b) Exposed 100 h in wet hydrogen at 1400°C.

Figure 13-Surface morphology of MgO.

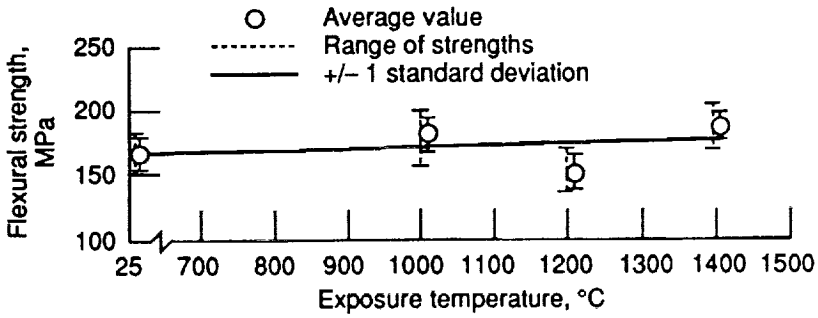

Figure 14-Effect of elevated temperature wet H_2 exposure (100 h) on room temperature strength of MgO.

Post-Exposure Strength of Magnesium Oxide. Room temperature strength of the MgO bars exposed to high-temperature wet H_2 is shown in Figure 14. The data indicate that the room temperature strength was essentially unaffected by the exposure. These results are somewhat unexpected since considerable surface attack was noted after the 1400°C exposure shown in Figure 13b. It is possible that internal flaws control the strength of the MgO tested. And even though the surface was altered by the H_2 exposure, the internal flaws may be more strength limiting than the surface flaws.

Mullite

Thermodynamic Stability of Mullite in Hydrogen. Misra (1) has described in detail the thermodynamic stability of mullite in H_2-containing environments. To summarize, the stability of mullite depends on the stability of its constituent oxides, Al_2O_3 and SiO_2. The equilibrium partial pressures of the gaseous products for the reaction of Al_2O_3 in $H_2 + H_2O$ are considerably lower than those for the reaction of SiO_2 in the same atmosphere. Thus, the reaction of the SiO_2 constituent is of primary concern in determining its stability in $H_2 + H_2O$ environments.

At high temperatures the primary gaseous product of the reaction of SiO_2 with H_2 is SiO, which forms according to the reaction

$$SiO_2 + H_2 = SiO + H_2O \qquad (7)$$

Figure 15 shows the equilibrium partial pressure of SiO(g) for the reaction of Equation 7 as a function of temperature and moisture level. On the basis of the stability criteria of 10^{-6} atmospheres of gaseous reaction product, the stability of mullite increases with increased moisture content. For example, mullite should be thermodynamically stable at 1400°C at moisture levels greater than 10 percent.

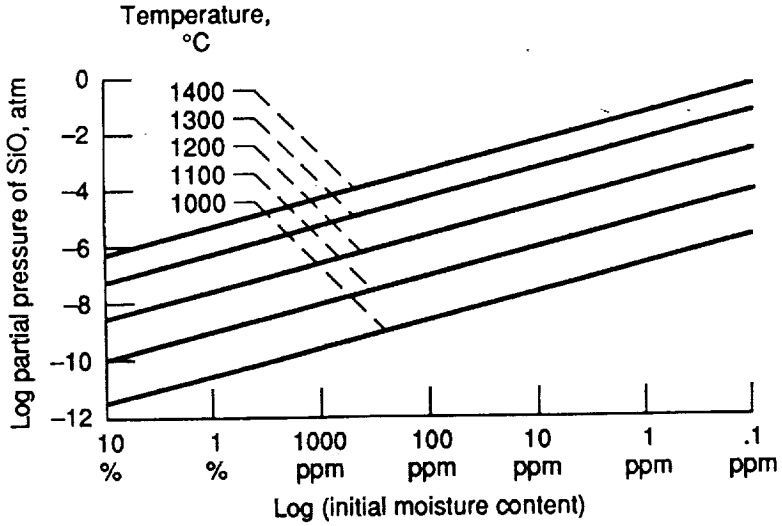

Figure 15-Partial pressure of SiO(g) as a function of moisture content and temperature for reaction of mullite with $H_2 + H_2O$ environments at a total pressure of 1 atm.

Morphology of Hydrogen Attack on Mullite. The removal of a glassy phase was the most obvious microstructural effect of high-temperature wet H_2 exposure of mullite. Representative surface morphologies are seen in Figure 16. Large voids are present in both the as-received and exposed microstructures. In Figure 16b the needlelike structure of the mullite grains is clearly visible. This is a result of the high-temperature H_2 environment removing the silica-rich intergranular glassy phase.

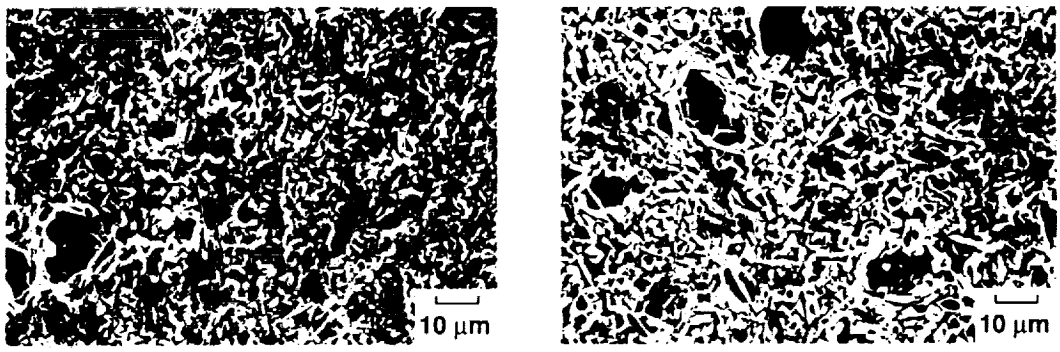

(a) As received. (b) Exposed 100 h in wet hydrogen at 1100°C.

Figure 16-Surface morphology of mullite.

Post-Exposure Strength of Mullite. A detailed evaluation of mullite exposed to dry H_2 and helium was conducted by Herbell et al. (11). They found that long exposure to dry H_2 at 1050°C and 1250°C severely degrades the strength of mullite. Exposure for 500 h at 1050°C produced a strength loss of 22 percent, and after 500 h at 1250°C the strength loss was greater than 50 percent. Post-exposure test bars of the same material exposed to wet H_2 for 100 h at temperatures to 1100°C are shown in Figure 17. The residual strength shows a steady decrease from 211 MPa in the as-received condition to about 180 MPa after exposure at 1100°C. This represents a strength loss of almost 14 percent after 100 h at only 1100°C.

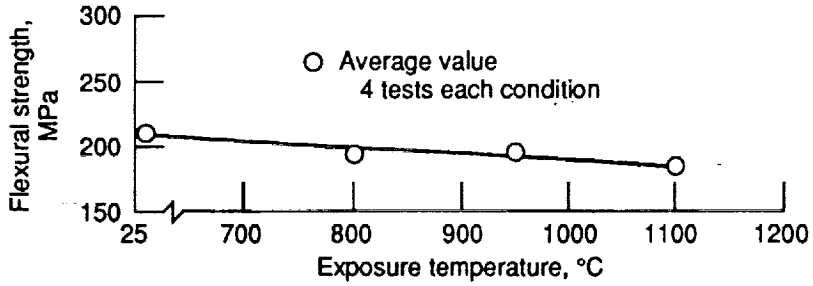

Figure 17-Effect of elevated temperature wet H_2 exposure (100 h) on room temperature strength of mullite.

Use Temperature Limits for Selected Ceramics in H_2-H_2O

The equilibrium thermodynamic stability of ceramic materials in H_2+H_2O atmospheres at high temperatures can be defined by selecting a limit of the partial pressure of reaction products present. For many applications the presence of 10^{-6} atm (1 ppm) of gaseous reaction product is reasonable. For other applications a higher or lower level may be the limiting condition for use. Figure 18 shows the projected stability of SiC, Si_3N_4, MgO, Al_2O_3, and mullite as a function of moisture content at 1 atm pressure based on 1 ppm of reaction product. As discussed, the stability of the SiO_2-forming (SiC and Si_3N_4) and SiO_2-containing (mullite) materials is determined primarily by the stability of SiO_2 in high temperature gaseous hydrogen. Pure H_2 is obviously a severe environment at high temperatures. The presence of water vapor improves the stability of many ceramics including those shown in the figure.

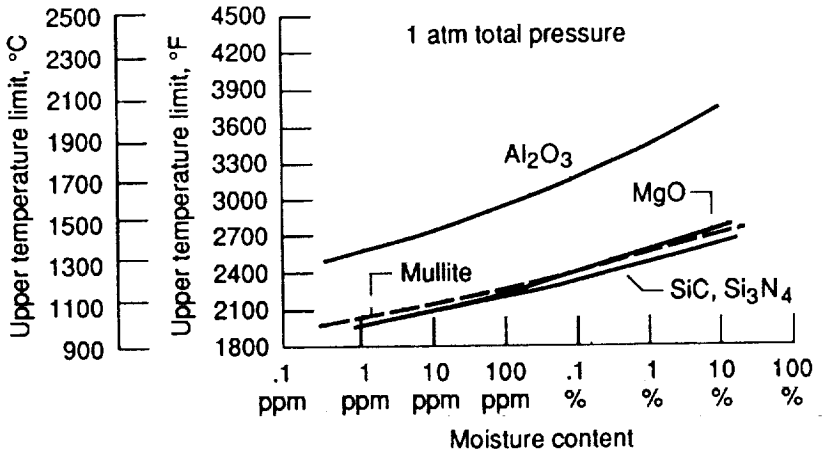

Figure 18-Upper temperature limit for ceramic materials in $H_2 + H_2O$ atmospheres.

Summary

The results of this study to evaluate the compatibility of selected ceramics in H_2 can be summarized as follows:

Silicon Carbide and Silicon Nitride

The thermodynamic upper use temperature for long-term stability of SiC and Si_3N_4 in wet H_2 is governed by stable SiO_2 scale formation. SiC is unstable in pure H_2, and the instability increases with temperature and pressure. Si_3N_4 decomposes in pure H_2 at temperatures above 1100°C.

Aluminum Oxide

The temperature limit of Al_2O_3 is in the 1200 to 1300°C range at 1-atm pressure in pure H_2. The thermodynamic stability of Al_2O_3 increases with moisture content, raising the upper use temperature to >1800°C at 10 percent moisture. However, changes in surface morphology may limit the structural integrity of Al_2O_3. There are no significant pressure effects at moderate moisture levels.

Magnesium Oxide

MgO has a thermodynamic stability to high-temperature H_2 exposure that is similar to SiC and Si_3N_4. Stability of MgO increases with moisture content and is unaffected by system pressure.

Mullite

Mullite stability in H_2-containing environments is controlled by the stability of the SiO_2. Stability in dry H_2 at high temperatures is poor. As with Al_2O_3, however, moisture improves the H_2 resistance of mullite and it should be stable -- at least for short exposure times to 900 to 1100°C with moisture levels greater than 10 percent.

Conclusions

In H_2O-containing H_2 environments, alumina is stable at temperatures >1800°C, and magnesia is stable to 1100 to 1200°C and may be used for short times at temperatures to 1400°C. Mullite is unstable and is severely attacked at temperatures as low as 1100°C. Silicon carbide and silicon nitride may be applicable for use in regimes where a stable silica layer forms on the surface. Although not considered as part of this study, it is obvious that the presence of impurities will play a role in the stability of ceramic materials in hydrogenous environments. Analysis of the effect of impurities and evaluation of the kinetics of a number of hydrogen-ceramic reactions is currently under study.

References

1. A. K. Misra, "Thermodynamic Analysis of Chemical Stability of Ceramic Materials in Hydrogen-Containing Atmospheres at High Temperatures" (NASA Contractor Report 4271, Sverdrup Technology Inc., Cleveland, Ohio, January 1990).

2. G. Eriksson, "Thermodynamic Studies of High Temperature Equilibriums. III SOLGAS, A Computer Program for Calculating the Composition and Heat Condition of an Equilibrium Mixture," Acta. Chem. Scand., 25(7)(1971), 2651-2658.

3. T. M. Besman, "SOLGASMIX-PV; A Computer Program to Calculate Equilibrium Relationships in Complex Chemical Systems" (Report ORNL/TM- 5775, Oak Ridge National Laboratory, Tennessee, 1977)

4. G. S. Fischman, S. D. Brown, and A. Zangvil, "Hydrogenation of Silicon Carbide: Theory and Experiments," Mat. Sci. and Eng., 72(1985), 295-302.

5. G. W. Hallum and T. P. Herbell, "Effect of High-Temperature Hydrogen Exposure on Sintered α-SiC," Adv. Ceram. Mat., 3(2)(1988), 171-175.

6. H. E. Kim, "Gaseous Corrosion of SiC and Si_3N_4 in Hydrogen" (Ph.D. thesis, Ohio State University, 1987).

7. N. S. Jacobson, et al., "Reactions of SiC With 5% H_2/Ar at 1300°C," J. Am. Ceram. Soc., 73(8)(1990), 2330-2332.

8. J. A. Costello and R. E. Tressler, "Oxidation Kinetics of Hot-Pressed and Sintered α-SiC," J. Am. Ceram. Soc., 64(6)(1981), 327-331.

9. E. A. Gulbransen and S. A. Jansson, "The High Temperature Oxidation, Reduction, and Volatilization Reactions of Silicon and Silicon Carbide," Oxid. Met., 4(3)(1972), 181-201.

10. G. C. Rybicki and J. L. Smialek, "Effect of the θ-α Al_2O_3 transformation on the Oxidation Behavior of β-NiAl+Zr," Oxidation of Metals, 31(3/4)(1989), 275-304.

11. T. P. Herbell, D. R. Hull, and G. W. Hallum, "Effect of High Temperature Hydrogen Exposure on the Strength and Microstructure of Mullite" (Paper presented at Fourth International Conference on Hydrogen Effects on Material Behavior, Moran, Wyoming, September 1989, to be published by TMS).

NASA
National Aeronautics and Space Administration

Report Documentation Page

1. Report No.	2. Government Accession No.	3. Recipient's Catalog No.
NASA TM-103674		

4. Title and Subtitle	5. Report Date
Effect of Hydrogen on the Strength and Microstructure of Selected Ceramics	6. Performing Organization Code

7. Author(s)	8. Performing Organization Report No.
Thomas P. Herbell, Andrew J. Eckel, David R. Hull, and Ajay K. Misra	E-5702
	10. Work Unit No. 582-01-11

9. Performing Organization Name and Address	11. Contract or Grant No.
National Aeronautics and Space Administration Lewis Research Center Cleveland, Ohio 44135-3191	13. Type of Report and Period Covered Technical Memorandum

12. Sponsoring Agency Name and Address	14. Sponsoring Agency Code
National Aeronautics and Space Administration Washington, D.C. 20546-0001	

15. Supplementary Notes

Prepared for the Fall Meeting of the Metallurgical Society, Detroit, Michigan, October 7-11, 1990. Thomas P. Herbell, Andrew J. Eckel, and David R. Hull, NASA Lewis Research Center. Ajay K. Misra, Sverdrup Technology, Inc., Lewis Research Center Group, 2001 Aerospace Parkway, Brook Park, Ohio 44142 (NASA Contract NAS3-25266). Responsible person, T.P. Herbell (216) 433-3246.

16. Abstract

Ceramics in monolithic form and as composite constituents in the form of fibers, matrices, and coatings are currently being considered for a variety of high-temperature applications in aeronautics and space. Many of these applications involve exposure to a hydrogen-containing environment. This study assesses the compatibility of selected ceramics in gaseous high-temperature hydrogen. Environmental stability regimes for the long term use of ceramic materials are defined by the parameters of temperature, pressure, and moisture content. Thermodynamically predicted reactions between hydrogen and several monolithic ceramics are compared with actual performance in a controlled environment. Morphology of hydrogen attack and the corresponding strength degradation is reported for silicon carbide, silicon nitride, alumina, magnesia, and mullite.

17. Key Words (Suggested by Author(s))	18. Distribution Statement
Ceramics Hydrogen Strength Microstructure	Unclassified – Unlimited Subject Category 27

19. Security Classif. (of this report)	20. Security Classif. (of this page)	21. No. of pages	22. Price*
Unclassified	Unclassified	15	A03

*For sale by the National Technical Information Service, Springfield, Virginia 22161